Proceedings World Geothermal Congress 2026
Calgary, Canada, June 8 – 11, 2026

Repeated Dike Intrusions as Heat Sources of Volcanic Geothermal Systems

Sigurður Ragnarsson[1]*, Gunnar Gunnarsson[2] and Magnús T. Gudmundsson[3]
Reykjavík Energy[1]*; Baseload Power Iceland[2]; Institute of Earth Sciences, University of Iceland[3]
sigurdur.ragnarsson@orkuveitan.is*

Keywords: Geothermal Reservoir, Heat sources, iTOUGH2, Numerical Modelling, Hengill, Volcano

ABSTRACT

The Hengill geothermal system in SW Iceland, 30 km east of Reykjavík, is a major energy source for the Capital Region. Operated by Reykjavík Energy's subsidiary ON Power, it hosts two co-generation plants with a combined capacity of 423 MWe and 540 MWth. Located within the rifting zone of the Mid-Atlantic Ridge, the nature of its heat sources remains uncertain. To explore the hypothesis that such systems can form via repeated shallow dike intrusions, a numerical modeling study was conducted. Using the iTOUGH2–EOS1sc module, which simulates water under sub- and supercritical conditions, a reservoir model was developed to 4 km depth, incorporating a permeability structure based on Hengill observations. Dike intrusions ~2 km long and ~25 m wide were simulated at depths between 1.2 and 3.0 km b.s.l., representing crustal extension over ~1,250 years. Results indicate that dikes reaching 2.5 km b.s.l. or higher, at 900°C and under lithostatic pressure, can generate temperature structures broadly consistent with those observed in the Hengill system within 5-10 thousand years, if they intersect permeable zones. These findings support the idea that high-temperature geothermal systems on divergent plate boundaries can form through repeated shallow diking, influencing the development and longevity of superheated zones.

1 INTRODUCTION

Geothermal resources are used worldwide for electricity generation and direct use, such as space heating and industrial processes. Although geothermal resources are considered sustainable, their long-term utilization depends on system characteristics and management, as production typically leads to reservoir pressure decline. Studies show that maintaining production below certain limits can allow for a balance between discharge and recharge, potentially sustaining utilization for 100–300 years (Axelsson, 2010). These findings are based on modeling constrained by geological, geochemical, and geophysical data, as well as production history (Steingrímsson, 2009; Axelsson, 2013).

Numerical modeling, particularly with codes such as TOUGH2 (Pruess et al., 2012), is widely used to simulate geothermal reservoir structures, conditions, and response to utilization. The iTOUGH2–EOS1sc module enables modeling of hydrothermal systems above the critical point of water, allowing for greater model depths and inclusion of hot formations like dikes or plutons (Magnusdottir & Finsterle, 2015).

The Hengill geothermal system in SW Iceland, about 30 km east of Reykjavík, is a major energy source for the capital region. ON Power operates two co-generation plants in the area with a total installed capacity of 423 MWe and 540 MWth (Gunnarsson et al., 2021). The system is located within the rifting zone of the Mid-Atlantic Ridge, and its heat sources are not fully understood. The area is characterized by basaltic rock formations, with increasing intrusion intensity at depth. Surface geothermal activity is common, but much of the alteration is fossil, indicating a more active system in the past (Franzson et al., 2010).

The general conceptual model for young igneous geothermal systems involves a heat source, permeable reservoir rocks, and a fluid phase, typically meteoric water (Stimac et al., 2015). In the Hengill area, resistivity and seismic studies indicate a clay cap at shallow depth, a high-resistivity core, and no current underlying magma chamber (Árnason et al., 2010; Franzson et al., 2010). The geothermal reservoir temperatures range from about 200°C to 320°C, with superheated conditions observed at depth in some wells.

Traditionally, geothermal reservoir models assume heat sources below the model depth, represented by boundary conditions (O'Sullivan & O'Sullivan, 2016). However, following deep drilling at IDDP-1, which encountered magma at 2.1 km depth (Friðleifsson et al., 2010), interest has grown in modeling shallow magmatic intrusions as heat sources. Gunnarsson and Aradóttir (2015) proposed that repeated shallow dike intrusions, rather than a large deep pluton, could explain the heat source in Hengill. Subsequent modeling using

the iTOUGH2–EOS1sc module has supported the idea that repeated diking can form high-temperature geothermal systems (Thorgilsson et al., 2018).

This study uses the iTOUGH2–EOS1sc module to further investigate whether repeated shallow dike intrusions can explain the observed temperature structure and heat flow in the Hengill geothermal system.

2 METHODS

2.1 Conceptual Model

The conceptual model is based on the divergent plate boundary in Iceland, which separates at an average rate of 2 cm/year. This rifting is assumed to be accommodated by repeated dike intrusions, each approximately 25 m thick and 2 km long, occurring every 1,250 years (Gunnarsson & Aradóttir, 2015). The permeability structure is based on the Hengill area, with a permeable upper crust to approximately 2.5 km depth, an impermeable cap rock at the top, and an impermeable base. The geothermal system is driven by thermal energy released from cooling dikes into the surrounding water-saturated host rock. Below 2.5 km, rocks are considered nearly impermeable, consistent with well data from the Hengill area (Gunnarsson & Aradóttir, 2015). The bottom boundary is set as nearly impermeable with a constant heat inflow of 210 mW/m^2, corresponding to a thermal gradient of 100°C/km (see Figure 1).

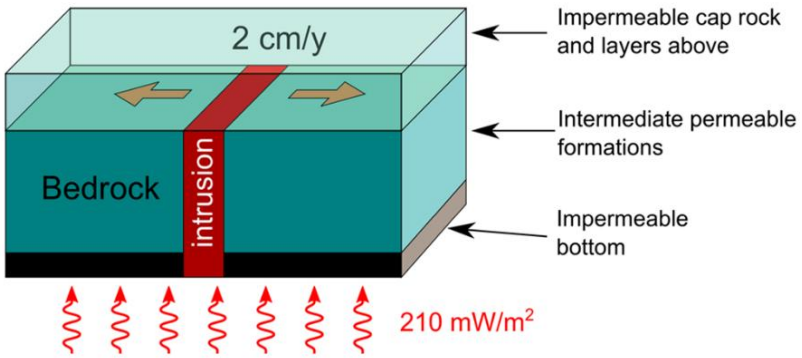


Figure 1. The conceptual model shown schematically. Two plates are separating at an average speed of 2 cm/year. At greater depths this gap is filled up with magma which forms dikes. The system has an impermeable bottom and heat flows into it from below. Adapted from Gunnarsson and Aradóttir (2015).

2.2 Numerical Methods

Numerical modeling was carried out using TOUGH2 with the iTOUGH2-EOS1sc module, which enables simulation of water under sub- and supercritical conditions (Magnusdottir & Finsterle, 2015; Pruess et al., 2012). Grids were generated with AMESH (Haukwa, 1998), and the models solve mass and energy balance equations using the integral finite difference method, with thermodynamic properties based on IAPWS standards (IAPWS, 2007, 2009).

2.3 Model Setup

The model domain covers 30 x 30 km laterally and extends to 4 km depth. A three-dimensional Voronoi grid was generated using the AMESH program, with finer resolution in the central area of interest. The grid consists of 12 vertical layers (A–L), with thickness ranging from 200 to 500 m (see Figure 2). Rock properties, including porosity and permeability, were assigned based on values calibrated for the Hengill area (Gunnarsson & Aradóttir, 2015) and are shown in Figure 3. The entire rock matrix is assumed to be is basalt with density 2,650 kg/m^3, heat conductivity 2.0 W/m/°C and specific heat 860 J/kg°C (Bruce & Huppert, 1990). Dikes are represented as narrow, high-temperature intrusions injected at intervals to simulate plate separation (see Figure 4). Dikes are assigned temperature-dependent permeability, decreasing log-linearly from host-rock values to 10^{-22} m^2 as temperature increases from 500°C to 960°C, to represent the transition from brittle to ductile behavior (Violay et al., 2012; Scott et al., 2018). This approach accounts for reduced permeability at high temperatures and enables simulation of transient heat transfer from cooling magma.

The top boundary is set as nearly impermeable with fixed temperature (15°C) and pressure (10 bar), while the bottom boundary has a constant heat flux. Lateral boundaries are modeled as large, low-permeability elements. Initial temperature and pressure distributions follow a geothermal gradient of 100°C/km and hydrostatic conditions, respectively.

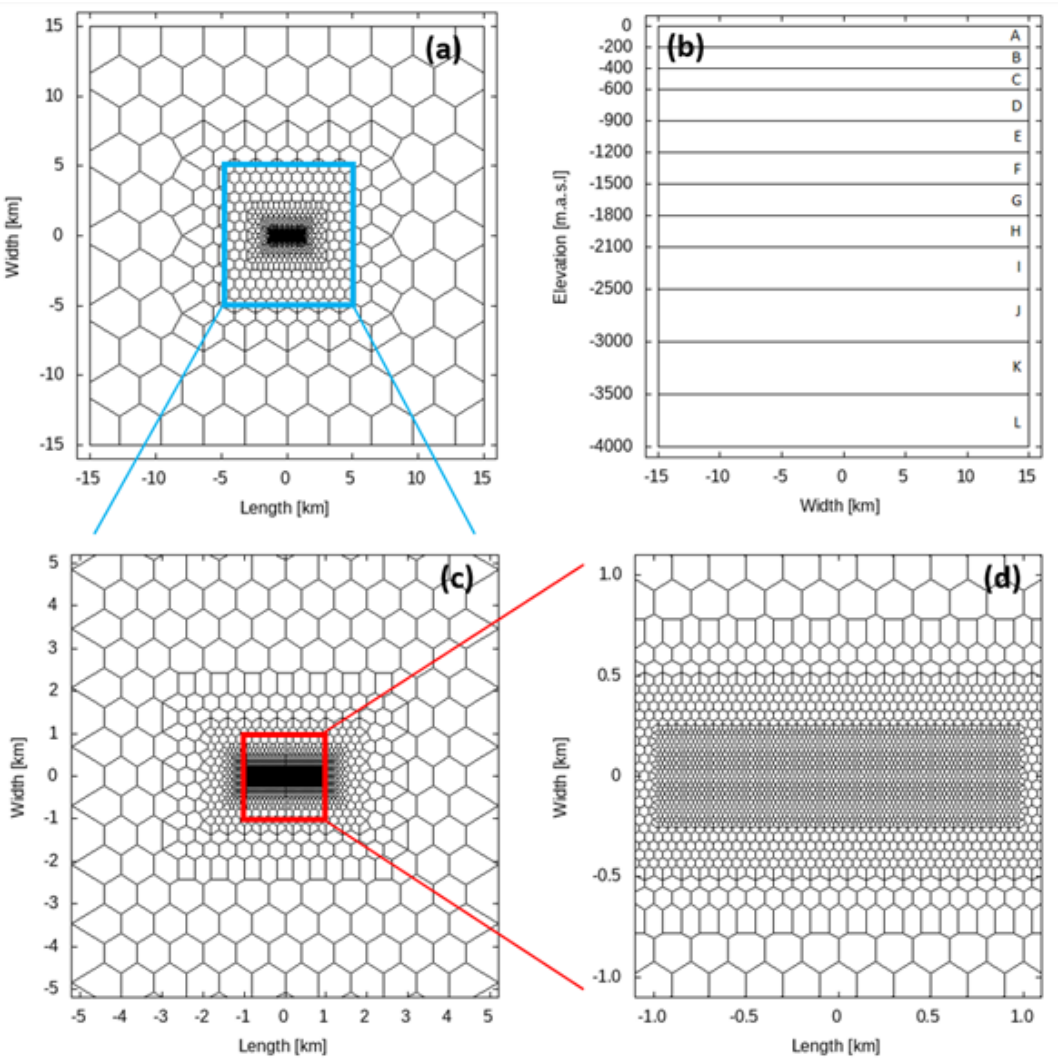
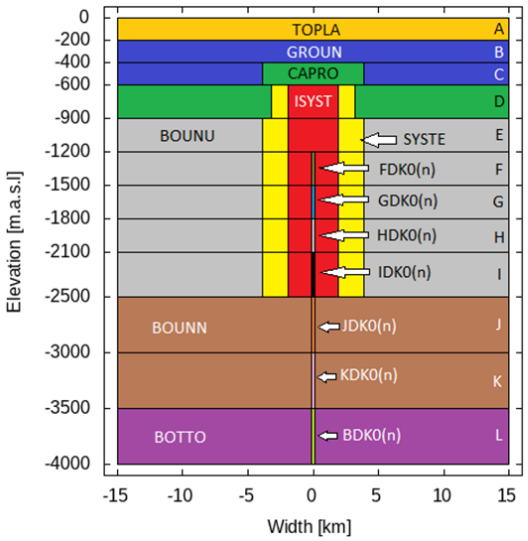


Figure 2. Horizontal Voroni grid generated by AMESH (a), (c), (d), with distance between element centers ranging from 25 to 3,200 m. (b) shows vertical layering structure of the model grid, the layers are named from A to L and their thickness ranges from 200 to 500 m.



Rock type	Porosity [%]	Permeability [m^2]
TOPLA	2.5	$1.0 \cdot 10^{-17}$
GROUN	5.0	$1.0 \cdot 10^{-15}$
CAPRO	2.5	$1.0 \cdot 10^{-17}$
SYSTE	10	$1.0 \cdot 10^{-16}$
ISYST	10	$1.0 \cdot 10^{-15}$
BOUNU	2.5	$5.0 \cdot 10^{-17}$
BOUNN	2.5	$5.0 \cdot 10^{-17}$
BOTTO	2.5	$1.0 \cdot 10^{-17}$
FDK(n)	2.5	$1.0 \cdot 10^{-15}$
GDK(n)	2.5	$1.0 \cdot 10^{-15}$
HDK(n)	2.5	$1.0 \cdot 10^{-15}$
IDK(n)	2.5	$1.0 \cdot 10^{-15}$
JDK(n)	2.5	$5.0 \cdot 10^{-17}$
KDK(n)	2.5	$5.0 \cdot 10^{-17}$
BDK(n)	2.5	$1.0 \cdot 10^{-17}$

Figure 3. Cross section through the middle of the model at length 0, showing the layering structure and distribution of rock types (labeled A–L) along with their porosity and permeability values. Rock types are marked by name and color, and *n* denotes dikes numbered 1–9 within each layer (see Figure 4 for dike placement).

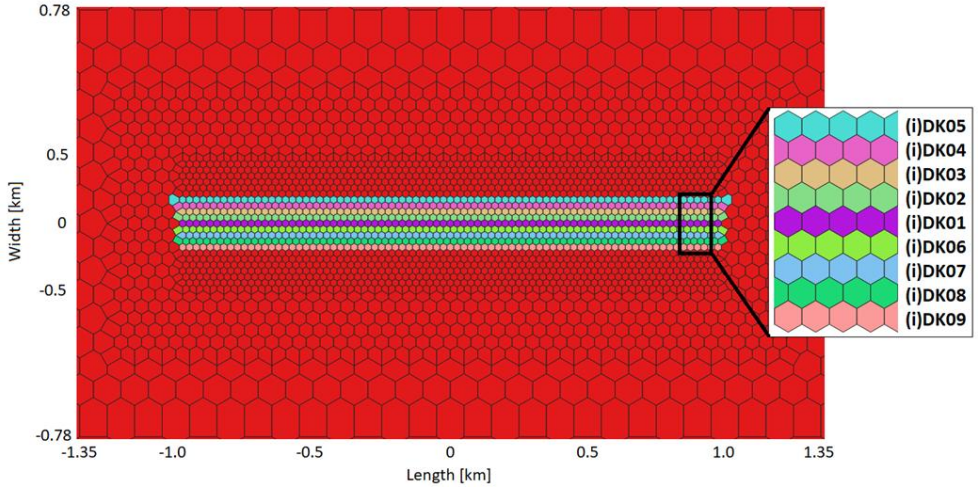


Figure 4. Innermost part of the model layers from F to L showing the location of the nine dikes. The inset shows the name of each dike with i denoting the corresponding layer. The rock properties of all the dikes in each layer are shown in Figure 3.

3 RESULTS

3.1 Diking Depth and System Development

Simulations were performed for repeated dike intrusions reaching different depths. When dikes intersected the permeable part of the system (up to layers F, G, H, I; 1.2–2.1 km), high-temperature geothermal systems (≥200°C at 1 km depth) developed within 2–6 thousand years, reaching steady-state temperatures of ~310°C at 1 km

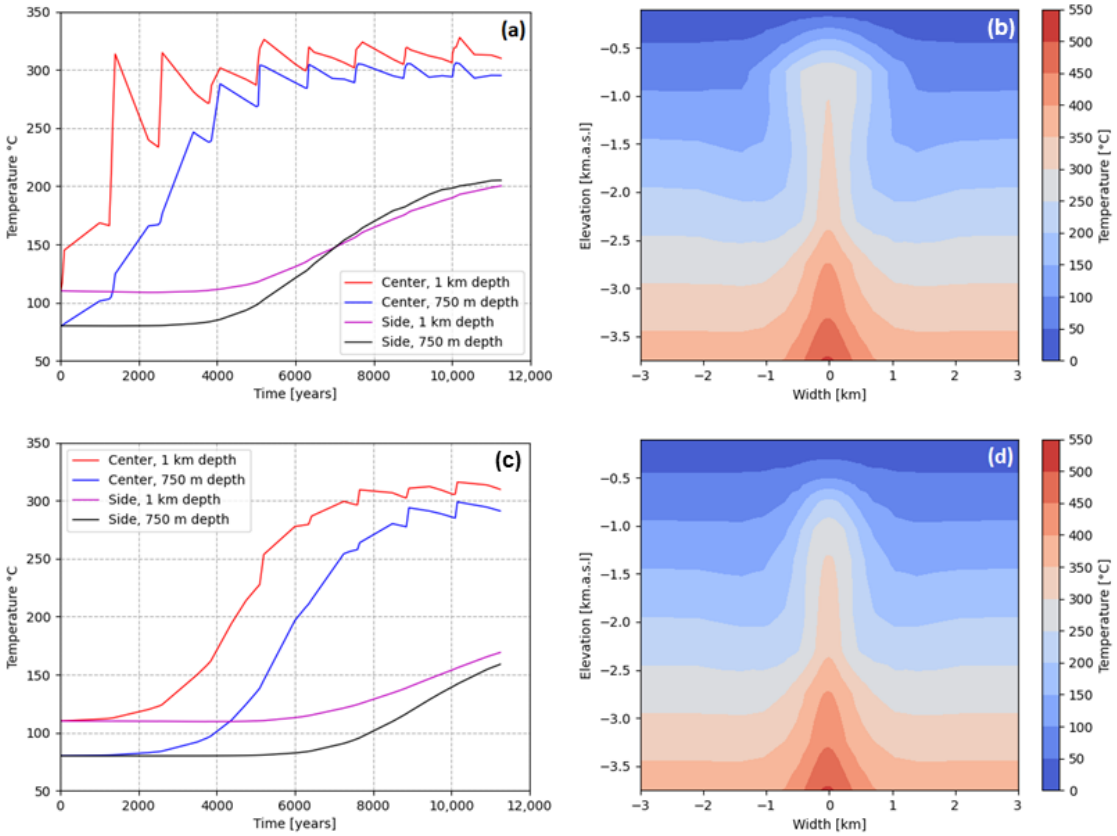


Figure 5.Temperature evolution (left) and temperature cross sections (right) for two diking scenarios into the permeable part: (a) and (b) show diking up to 1.2 km depth and (c) and (d) up to 2.1 km depth. Time-series plots show temperature at four locations at 1 km and 750 m depth, and the same depths 1 km outside the diking area. Cross sections represent the thermal structure through the model center (length = 0 km) after 6,250 years.

depth in the center after 5-8 thousand years (see Figure 5). The size and evolution of the temperature anomaly depend on both time and the height reached by diking from below. Once the center stabilizes with ~310°C at 1 km depth, additional energy expands the heated region and widens convection cells. At 6,250 years, cross sections show temperatures of 250-350°C in the upper permeable part, similar to those observed in high-temperature geothermal systems such as Hengill. The width of the warm zone and the overall temperature structure increase as dikes reach higher into the permeable part of the system. The higher the dikes go, the faster and broader the temperature anomaly develops, as expected, since energy injection correlates with the mass of magma injected into the system.

Diking up to the base of the permeable part (layer J; 2.5 km) produces a high-temperature system, with temperatures in the center reaching ~300°C after 11,250 years. The temperature anomaly is narrower than for diking into the permeable part, and lateral heating starts 2-4 thousand years later (see Figure 6). Diking below the permeable part (layer K; 3 km) does not form a high-temperature system within the simulation period, though temperatures began to rise at the center (see Figure 7). The difference can be explained by two factors, where higher-reaching dikes inject more energy and cooling dikes within permeable host rock transfer heat faster because convective circulation dominates in permeable zones, unlike in near impermeable formations where heat transfer is primarily conductive.

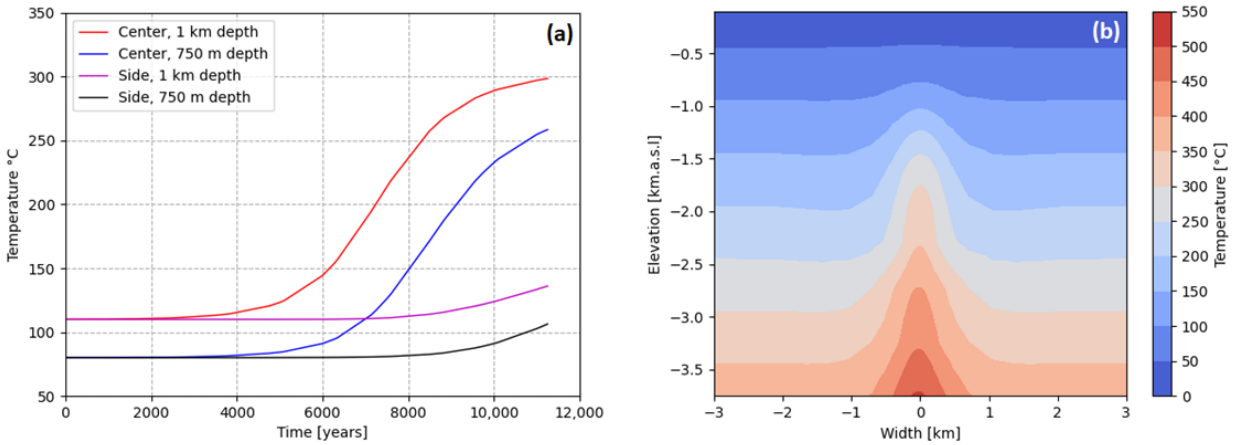


Figure 6. Temperature evolution for diking up to depth of 2.5 km, reaching the base of the permeable part. (a) Time-series at four locations: center at 1 km and 750 m depth, and at the same depths 1 km outside the diking area. (b) Temperature cross section through the model center (length = 0 km) at 6,250 years.

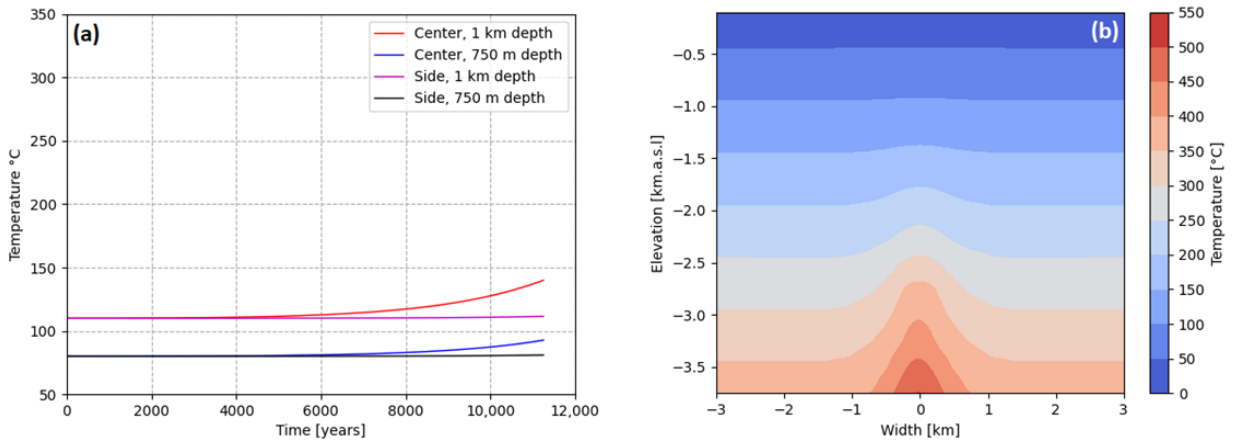


Figure 7. Temperature evolution for diking up to depth of 3 km, not reaching the base of the permeable part. (a) Time-series at four locations: center at 1 km and 750 m depth, and at the same depths 1 km outside the diking area. (b) Temperature cross section through the model center (length = 0 km) at 6,250 years.

3.2 The Effects of Host-Rock Permeability

The effects of host-rock permeability were studied by using the model assuming diking up to layer H at 1.8 km depth as a study case. The permeability of the rock types ISYST and the dikes in the permeable part with rock

types HDK(n) and IDK(n) were varied from the original values (see Figure 3). Two simulations were performed, one where the permeability of the rock types was decreased by half to $0.5 \cdot 10^{-15}$ m^2 and another one where it was increased by a factor of two, to $2.0 \cdot 10^{-15}$ m^2.

Varying the permeability of the host rock (ISYST, HDK(n), IDK(n)) showed that higher permeability led to faster system development but lower steady-state temperatures, while lower permeability delayed system development but resulted in higher central temperatures (see Figure 8). Simulation instability limited the lowest permeability case to 8,750 years, but trends were clear.

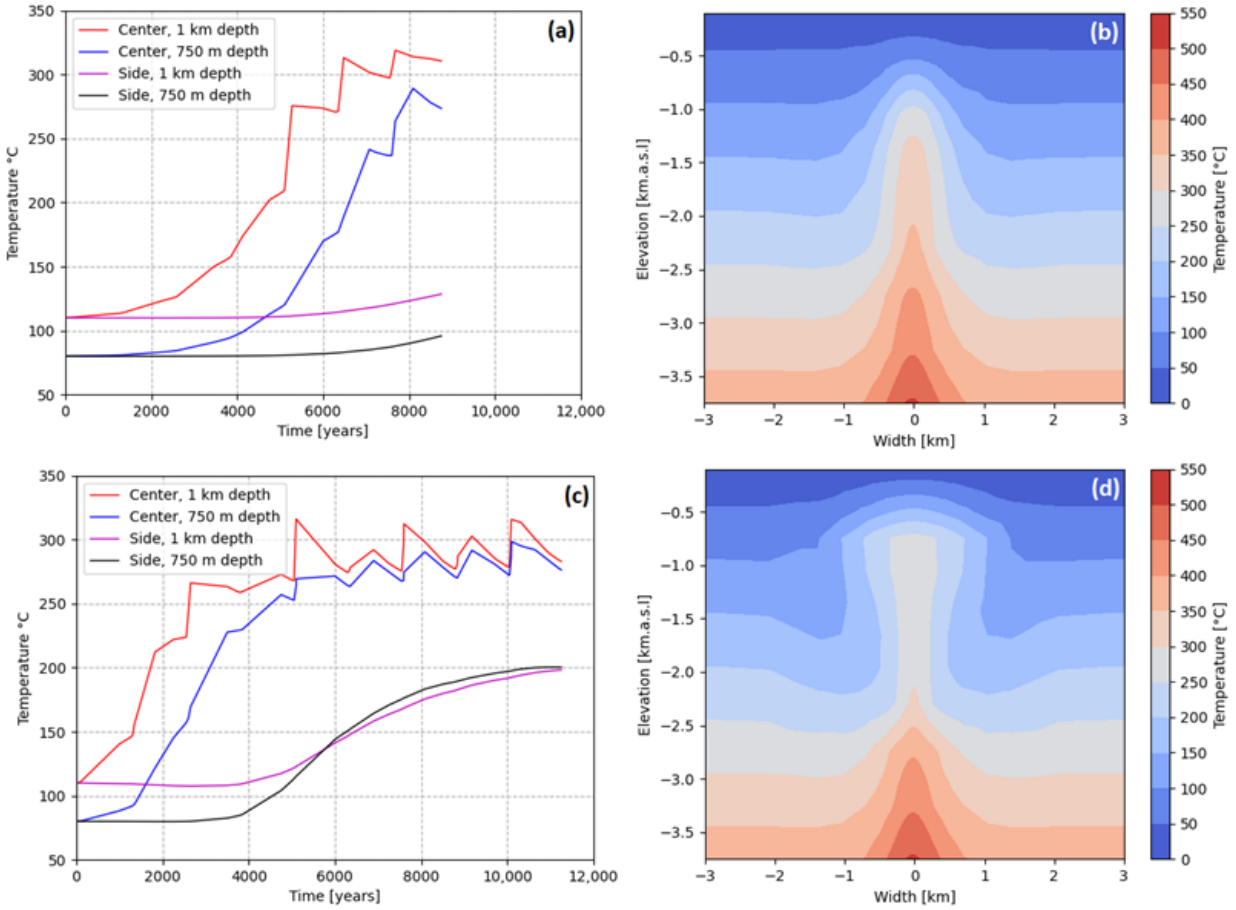


Figure 8. Temperature evolution at four different locations in the model and temperature cross section at length = 0 km, for diking up to 1.8 km depth. With permeability of the rock types ISYST, HDK(n) and IDK(n) given in Figure 3, decreased by half (a) and (b) and increased by a factor of two (c) and (d).

3.3 Post-Diking Evolution

The system developed with diking up to 1.8 km depth was simulated for another 40,000 years after dike intrusions stopped, following 10,000 years of repeated diking (a total of nine diking events). Figure 9 shows the temperature evolution of the system. A meta steady state with temperature ~310°C in the center at 1 km depth is reached after ~5,000 years of diking and persists until diking ceases. After diking stops, the center cools rapidly by ~60°C in the first 10,000 years and then gradually another ~40°C over the next 30,000 years. At 49,000 years, the system still qualifies as high-temperature system (>200 °C at 1 km depth), though its structure differs from the warmest period (~11,250 years).

After the nine diking events ended, the center cooled, while lateral heating continued for another 2-5 thousand years, indicating that the system continued to grow laterally during that period. The maximum size was reached at ~15,250 years, with temperatures of ~270°C at the center and ~190°C 1 km to the side at 1 km depth. This behavior shows that even after diking stops, thermal evolution remains dynamic, with lateral expansion continuing beyond the peak heating phase of the center.

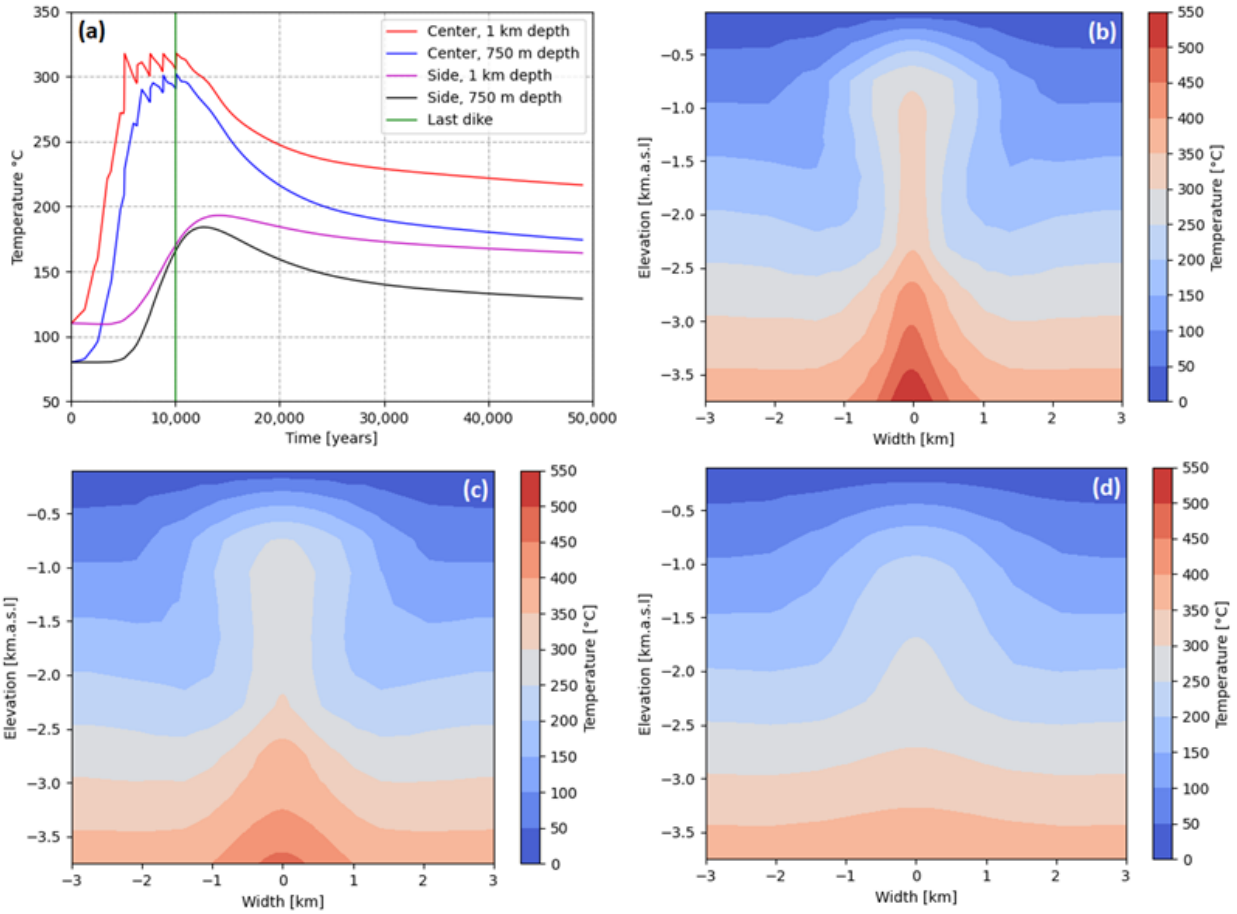


Figure 9. Temperature evolution at four different locations in the model (a) and temperature cross sections at length = 0 km, for diking up to 1.8 km depth. The cross sections show the state after 11,250 years (b), 15,250 years (c) and 49,000 years (d).

3.4 System Flow Dynamics and Phase Conditions

Streamline analysis for simulations with repeated diking up to and into the permeable part of the system showed the development of symmetrical convection cells in the permeable part, with up-flow at the center. Differences in streamline trends are expected in a small region near the center shortly after a dike intrudes into the permeable part, as the dike and its contact surfaces with the host rock remain near impermeable while temperatures exceed ~500°C.

Pressure in the center was slightly above hydrostatic, likely due to the cap rock sealing the system. Attempts to vent through small permeable zones had minor effects, so the system was kept closed.

Figure 10 shows temperature and steam ratio for diking up to 1.8 km after 8,850 years (100 years post-diking episode 8). The diking zone was still cooling, with temperatures up to 550°C at 2 km depth and high steam ratio near the dike. A narrow two-phase band extended to the cap rock at ~600 m depth, and a larger steam zone occurred below 2.5 km in near impermeable formations.

Systems with diking into the permeable part were mainly liquid dominated, except near or above dikes for ~150 years after diking. Steam zone size and duration depend on system temperature and permeability, lower permeability favors steam formation. For diking only up to the base of the permeable part (2.5 km), no steam developed within the permeable zone during the 11,250 years simulation. Both scenarios produced superhot steam zones below 2.5 km, but these are impractical to exploit in a conventional manner due to low permeability. However, they might become economically feasible with advancements in superhot EGS technology.

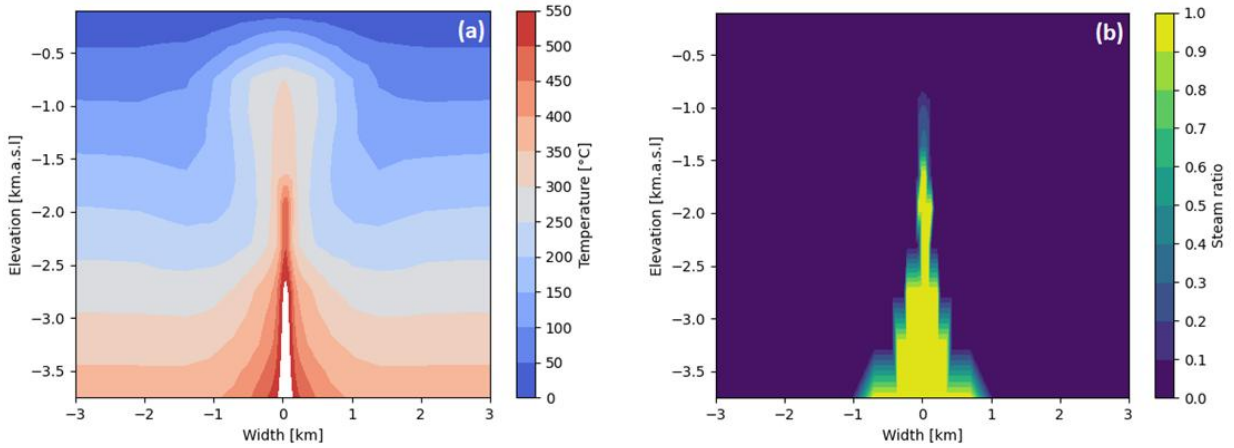


Figure 10. Temperature (a) and steam ratio (b) cross sections at length = 0 km for diking up to 1.8 km depth after 8,850 years (100 years post-diking episode 8). White in (a) indicates temperatures above 550°C.

3.5 Heat Flow at 2.1 km Depth

Figures 11a and b show heat flow at 2.1 km depth, from layer I to layer H (see Figure 3), similar to the depth where heat and mass are injected in Reykjavík Energy´s Hengill reservoir model (Gunnarsson, pers. comm., 2022). The highest heat flow, up to 24 W/m^2, occurs in an elliptical zone above the diking area at the center of the model.

Figure 11b shows heat flow evolution through a 1 x 0.5 km area at 2.1 km depth in the center of the model for both diking up to the base of the permeable part (2.5 km depth), as well as diking into the permeable part (1.8 km depth). For diking up to the base of the permeable part, heat flow rises to ~10 MW (average flux ~20 W/m^2) after 7,600 years and ~12 MW (average flux ~24 W/m^2) after 11,250 years. Diking into the permeable part shows a similar trend but oscillates, briefly doubling heat flow at 2.1 km depth after intrusion at 1.8 km.

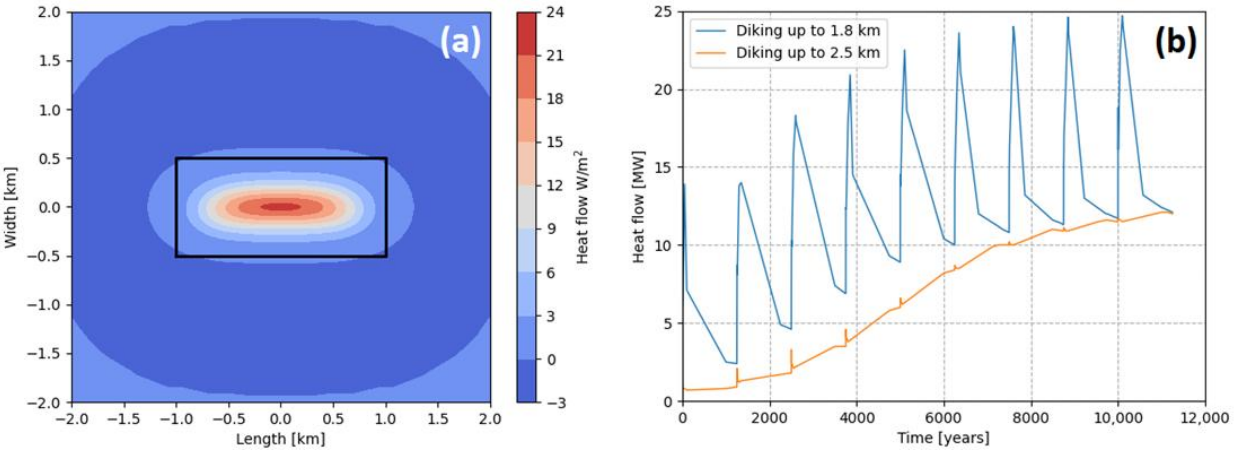


Figure 11. Heat flow at 2.1 km depth, from layer I up to layer H after 11,250 years: (a) diking up to 2.5 km depth; black box marks are used for total heat flow calculation. (b) Time evolution of heat flow for diking up to 2.5 km and 1.8 km depth.

4 DISCUSSION

4.1 Model Results and Assumptions

Numerical modeling suggests repeated diking can form high-temperature geothermal systems within 5-10 thousand years, if intrusions reach permeable zones. These systems are mainly liquid dominated, with transient steam zones near the cooling dikes for ~150 years. Heat flow across a 1 x 0.5 km surface at 2.1 km depth reaches 10-12 MW, briefly peaking at ~25 MW during shallow diking.

Unlike conventional reservoir models focused on production zones (O'Sullivan & O'Sullivan, 2016), this study modeled the entire system using dikes as heat sources. Assumptions include a pre-existing permeability structure and cap rock, as seen in the Hengill area, implying a previously cooled system undergoing renewed magmatism. Absence of a cap rock would delay system development due to convective heat loss.

Permeability below 2.5 km was assumed negligible, consistent with intrusive dominance in Hengill wells (Franzson et al., 2010; Ingebritsen & Manning, 2010). However, this depth is probably variable between areas, e.g. IDDP-2 indicates deeper feed zones in the Reykjanes system (Friðleifsson et al., 2020). Nine dikes (~25 m wide, ~2 km long) were emplaced at 1,250-year intervals, with temperatures set to 900°C and lithostatic pressure. Heat transfer assumptions followed Scott et al. (2015, 2016) and Thorgilsson et al. (2018), accounting for brittle-ductile temperature (BDT) by reducing permeability log-linearly above it and doubling heat capacity to include latent heat of crystallization. Heat moves by conduction above BDT and convection below, enabling groundwater to mine dike heat. Other magmatic processes were neglected, but this approximates transient heat transfer from cooling magma by using TOUGH2 and the iTOUGH2-EOS1sc module.

Geodynamic effects of rifting (~225 m over 11,250 years) were ignored, though they likely alter permeability and flow paths. The model used thinner dikes (~25 m) than prior studies (500 m and 230 m; Gunnarsson & Aradóttir, 2015; Thorgilsson et al., 2018). This better approximates the rifting style represented in our conceptual model while increasing simulation time. The total simulation duration was 11,250 years, which is consistent with previous findings that geothermal systems can form within 2-10 thousand years (Scott et al., 2016).

4.2 Heat Sources of the Hengill System

The absence of a large magmatic body beneath Hengill challenges earlier views of a central convection cell with Nesjavellir and Hellisheiði in the outflow zones. Borehole data and reservoir models suggest localized up-flow zones in fissure swarms, likely due to permeability anomalies or shallow intrusions (Gunnarsson & Aradóttir, 2015).

In this study´s model, >250°C zone at 1 km depth cover ~1-2 km^2 for diking up to 2.5 km and 1.8 km depth, compared to ~4 km^2 in Nesjavellir. Heat flow at 2.1 km depth after 11,250 years is 10-12 MW, briefly doubling after shallow diking, versus ~33 MW in Reykjavík Energy's reservoir model (Gunnarsson, pers. comm., 2022). Although simplified, results support the hypothesis that repeated shallow intrusions can form and sustain geothermal systems on divergent plate boundaries. Longer simulations with more diking events and longer dikes are expected to improve agreement with field observations.

5 CONCLUSIONS

A numerical modeling study using TOUGH2 and the iTOUGH2–EOS1sc module was conducted to investigate whether repeated shallow dike intrusions can account for the heat source and temperature structure observed in high-temperature geothermal systems, such as in the Hengill area in SW Iceland. The results show that intrusions reaching into or near the permeable part of the system can generate and sustain high-temperature geothermal reservoirs within 5-10 thousand years, producing temperature and heat-flow patterns broadly consistent with field observations. Although the modeled values are somewhat lower than those measured in the Nesjavellir field, extending simulations to include more diking events and longer dikes is expected to improve agreement with field data. Overall, the findings support the hypothesis that repeated shallow magmatic intrusions are a plausible mechanism for the formation and maintenance of high-temperature geothermal systems on divergent plate boundaries, influencing their development and longevity.

Acknowledgements

This paper is based on research conducted for the author's MS thesis at the University of Iceland, prior to employment at Reykjavík Energy. The author thanks the Division of Research and Innovation at Reykjavík Energy for support with facilities, equipment, and data, and acknowledges Dr. Þorvarður Árnason for assistance in securing research funding from the University of Iceland.

REFERENCES

Árnason, K., Eysteinsson, H., and Hersir, G.P.: Joint 1D inversion of TEM and MT data and 3D inversion of MT data in the Hengill area, SW Iceland, Geothermics, 39, (2010), 13–34.

Axelsson, G.: Sustainable geothermal utilization – Case histories; definitions; research issues and modelling, Geothermics, 39, (2010), 283–291.

Axelsson, G.: Dynamic modelling of geothermal systems, Short Course V on Conceptual Modelling of Geothermal Systems, UNU-GTP and LaGeo, (2013).

Bruce, P.M., and Huppert, H.E.: Magma transport and storage, In Ryan, M.P. (Ed.), Magma Transport and Storage, John Wiley & Sons Ltd., (1990), 87–101.

Franzson, H., Gunnlaugsson, E., Árnason, K., Sæmundsson, K., Steingrímsson, B., and Harðarson, B.S.: The Hengill Geothermal System, Conceptual Model and Thermal Evolution, Proceedings, World Geothermal Congress, Bali, Indonesia, (2010).

Friðleifsson, G.Ó., Albertsson, A., and Elders, W.A.: Iceland Deep Drilling Project IDDP – 10 Years Later – Still an Opportunity for International Collaboration, Proceedings, World Geothermal Congress, Bali, Indonesia, (2010).

Friðleifsson, G.Ó., Elders, W.A., Zierenberg, R.A., Fowler, A.P.G., Weisenberger, T.B., Mesfin, K.G., Sigurðsson, Ó., Níelsson, S., Einarsson, G., Óskarsson, F., Guðnason, E., Tulinius, H., Hokstad, K., Benoit, G., Nono, F., Loggia, D., Parat, F., Cichy, S.B., Escobedo, D., and Mainprice, D.: The Iceland Deep Drilling Project at Reykjanes: Drilling into the root zone of a black smoker analog, Journal of Volcanology and Geothermal Research, 391, (2020)

Gunnarsson, G., and Aradóttir, E.S.P.: The Deep Roots of Geothermal Systems in Volcanic Areas: Boundary Conditions and Heat Sources in Reservoir Modeling, Transport in Porous Media, 108, (2015), 43–59.

Gunnarsson, G., Tómasdóttir, S., Klüpfel, S., Westergren, Á., and Björnsson, G.B.: Managing the Production Fields in the Hengill Area, Proceedings, World Geothermal Congress 2020+1, Reykjavik, Iceland, (2021).

Haukwa, C.B.: AMESH – A Mesh Creating Program for the Integral Finite Difference Method, Lawrence Berkeley National Laboratory, (1998).

IAPWS: Revised Release on the IAPWS Industrial Formulation 1997 for the thermodynamic properties of water and steam, The International Association for the Properties of Water and Steam, (2007).

IAPWS: Revised Release on the IAPWS Formulation 1995 for the thermodynamic properties of ordinary water substance for general and scientific use, The International Association for the Properties of Water and Steam, (2009)

Ingebritsen, S.E., and Manning, C.E.: Permeability of the continental crust: Dynamic variations inferred from seismicity and metamorphism, Geofluids, 10, (2010), 193–205.

Magnusdottir, L., and Finsterle, S.: iTOUGH2-EOS1 SC: Multiphase Reservoir Simulator for Water under Sub- and Supercritical Conditions – User's Guide, Lawrence Berkeley National Laboratory, (2015).

O'Sullivan, M.J., and O'Sullivan, J.P.: Reservoir modeling and simulation for geothermal resource characterization and evaluation, in Geothermal Power Generation: Developments and Innovation, Elsevier Ltd., (2016).

Pruess, K., Oldenburg, C., and Moridis, G.: TOUGH2 User's Guide, Version 2, Lawrence Berkeley National Laboratory, (2012).

Scott, S., Driesner, T., and Weis, P.: Geologic controls on supercritical geothermal resources above magmatic intrusions, Nature Communications, (2015).

Scott, S., Driesner, T., and Weis, P.: The thermal structure and temporal evolution of high-enthalpy geothermal systems, Geothermics, 62, (2016), 33–47.

Scott, S., Driesner, T., and Weis, P.: A New Conceptual Framework for the Deep Roots of Magma-Driven Geothermal Systems, Proceedings, 43rd Workshop on Geothermal Reservoir Engineering, Stanford, California, (2018).

Steingrímsson, B.: Geothermal Exploration and Development From a Hot Spring To Utilization, Short Course on Surface Exploration for Geothermal Resources, UNU-GTP and LaGeo, (2009).

Stimac, J., Goff, F., Goff, C.J: Chapter 46: Intrusion-related geothermal systems. In: Encyclopedia of Volcanoes, Elsevier, Editors: Sigurdsson, H., Houghton, B., McNutt, S.R., J. Stix, 799-822 (2015).

Thorgilsson, G., Axelsson, G., Berthet, J.C., Magnúsdóttir, L., and Árnason, K.: Modelling of the Deep Roots of Volcanic Geothermal Systems, Proceedings, 43rd Stanford Geothermal Workshop, Stanford, California, (2018).

Violay, M., Gibert, B., Mainprice, D., Evans, B., Dautria, J.-M., Azais, P., and Pezard, P.: An experimental study of the brittle-ductile transition of basalt at oceanic crust pressure and temperature conditions, Journal of Geophysical Research: Solid Earth, 117(3), (2012). https://doi.org/10.1029/2011JB008884